Biochimica et Biophysica Acta 1838 (2014) 1922–1930

Contents lists available at ScienceDirect

Biochimica et Biophysica Acta

journal homepage: www.elsevier.com/locate/bbamem

Sphingolipid symmetry governs membrane lipid raft structure

Peter J. Quinn *

Department of Biochemistry, King's College London, 150 Stamford Street, London SE1 9NH, UK

ARTICLE INFO

Article history:
Received 20 January 2014
Received in revised form 24 February 2014
Accepted 27 February 2014
Available online 7 March 2014

Keywords:
Raft
Membrane raft
Lipid bilayer structure
Cholesterol
Sphingomyelin
Glycosphingolipid

ABSTRACT

Lipid domain formation in membranes underlies the concept of rafts but their structure is controversial because the key role of cholesterol has been challenged. The configuration of glycosphingolipid receptors for agonists, bacterial toxins and enveloped viruses in plasma membrane rafts appears to be an important factor governing ligand binding and infectivity but the details are as yet unresolved. I have used X-ray diffraction methods to examine how cholesterol affects the distribution of glycosphingolipid in aqueous dispersions of an equimolar mixture of cholesterol and egg-sphingomyelin containing different proportions of glucosylceramide from human extracts. Three coexisting liquid-ordered bilayer structures are observed at 37 °C in mixtures containing up to 20 mol% glycosphingolipid. All the cholesterol was sequestered in one bilayer with the minimum amount of sphingomyelin (33 mol%) to prevent formation of cholesterol crystals. The other two bilayers consisted of sphingomyelin and glucosylceramide. Asymmetric molecular species of glucosylceramide with N-acyl chains longer than 20 carbons form an equimolar complex with sphingomyelin in which the glycosidic residues are arranged in hexagonal array. Symmetric molecular species mix with sphingomyelin in proportions less than equimolar to form quasicrystalline bilayers. When the glycosphingolipid exceeds equimolar proportions with sphingomyelin cholesterol is incorporated into the structure and formation of a gel phase of glucosylceramide is prevented. The demonstration of particular structural features of ceramide molecular species combined with the diversity of sugar residues of glycosphingolipid classes paves the way for a rational approach to understanding the functional specificity of lipid rafts and how they are coupled across cell membranes.

1. Introduction

A universal feature of cell receptor and signalling processes is the assembly of recognition and associated transducing elements in the lipid bilayer matrix of the membrane. The structural role of lipids in receptor functions is conjectural. While the biochemical machinery responsible for creating and maintaining lipid asymmetry across the bilayer membrane is reasonably well understood [1] the factors underlying lateral domain formation and coupling are more problematic. There is abundant evidence from the dynamics of fluorescent lipid probes on the surface of living cells that domains differing in lipid motion or fluidity exist and particular lipid classes are known to partition into domains [2,3]. The creation of these membrane domains must involve specific interactions between different membrane constituents but at present there is uncertainty with regard to the extent to which protein–lipid interactions or interactions between different lipids govern the process. Specific membrane lipid binding motifs, for example, have been identified in transmembrane segments of intrinsic proteins [4] while interaction between cytoplasmic proteins and membrane lipids in such processes as assembly of viral envelopes has yet to be resolved [5].

One model to explain domain formation is the lipid raft hypothesis which, as originally postulated [6] and subsequently refined [7,8], envisages the driving force as preferential interactions between cholesterol and saturated molecular species of lipid of which sphingolipids are the most abundant. The resulting liquid-ordered phase is said to be thicker than the coexisting liquid-disordered phase contributing further to lateral phase separation through hydrophobic mismatch. The key role attributed to cholesterol in animal and other sterols in plant and microbial membranes [9] in creation of lipid raft domains, however, is not consistent with the data derived from both model and cellular systems nor the range of molecular species of lipids present in cell membranes.

The interaction of cholesterol and other membrane lipids to create domain structures appears to be a much more specific process than hitherto envisaged. Cholesterol, for example, preferentially interacts with symmetric molecular species of sphingomyelin [10–12] particularly N-palmitoyl sphingomyelin [13] and forms a stoichiometric complex with symmetric sphingomyelin at physiological temperatures [14,15]. Cholesterol, on the other hand, is immiscible with glycosphingolipids at 37 °C [16]; this is at odds with the essential role such lipids are known to perform in raft-mediated signalling processes [17,18]. There is also evidence from high resolution (87 nm) secondary ion mass spectrometry mapping of the distribution of cholesterol and sphingolipids in the plasma membrane of fibroblasts that the two

* Tel.: +44 2078484408; fax: +44 2078484500.
E-mail address: p.quinn@kcl.ac.uk.

http://dx.doi.org/10.1016/j.bbamem.2014.02.021
0005-2736/

lipids are not co-localized [19]. This led to the conclusion that favourable sphingolipid–cholesterol interactions do not dictate membrane organization. Furthermore, the notion that hydrophobic mismatch contributes to lateral phase separation of raft components is not consistent with a failure to distinguish a significant difference between the thickness sphingomyelin–cholesterol complexes and pure phospholipid bilayers [15] or membrane rafts and the plasma membranes from which they were derived [20].

The conventional approach to model the creation of liquid-ordered structures in ternary lipid mixtures has been to focus on how cholesterol interacts with phospholipids with relatively high and low phase transition temperatures [21,22]. Molecular species of sphingomyelin commonly found in cell membranes forms stoichiometric complexes with cholesterol [15] and these complexes phase separate in fluid phospholipid bilayers [14]. To investigate how cholesterol distributes between different sphingolipids I examined the structure of aqueous dispersions of equimolar mixtures of cholesterol and egg-sphingomyelin containing different amounts of glucosylceramide using X-ray diffraction methods. Three discrete bilayer structures were formed in the ternary lipid mixtures. Cholesterol was present in only one structure together with the minimum amount of sphingomyelin needed to prevent phase separation of crystalline cholesterol. The other two bilayers also contained sphingomyelin, one consisting of a 1:1 stoichiometric complex with molecular species of glucosylceramide with N-acyl fatty acids longer than 20 carbon atoms and the other with symmetric molecular species of glucosylceramide.

2. Methods

2.1. Lipids

Chicken egg sphingomyelin (eggSM) was purchased from Avanti Polar Lipids (Alabaster, AL). This source of sphingomyelin is predominantly amidified with palmitic acid (65%) and there are relatively smaller amounts of stearic and very long-chain fatty acids (C22:0, C24:0, C24:1; <10%). A mean molecular weight of 712 g/mol was used. Cholesterol was purchased from Sigma-Aldrich (UK). Natural cerebroside, ceramide β-D glucoside (GluCer) extracted from the spleen of patients with Gaucher's disease was purchased from Matreya Inc. (Pleasant Gap, PA) and used without further purification. GluCer was >98% pure as judged by thin-layer chromatography and a mean molecular weight of 779 g/mol was used.

2.2. Sample preparation

Samples for X-ray diffraction examination were prepared by dissolving lipids in warm (45 °C) chloroform/methanol (2:1, vol/vol) and mixing them in the desired proportions (denoted as mol GluCer/100 mol eggSM + cholesterol + GlcCer). The solvent was subsequently evaporated under a stream of oxygen-free dry nitrogen at 45 °C and any remaining traces of solvent were removed by storage under high vacuum for two days at 20 °C. The dry lipids were hydrated with deionized water to give a dispersion of 25 wt.% lipid. This was sufficient for full hydration of the lipids. The lipids were stirred thoroughly with a thin

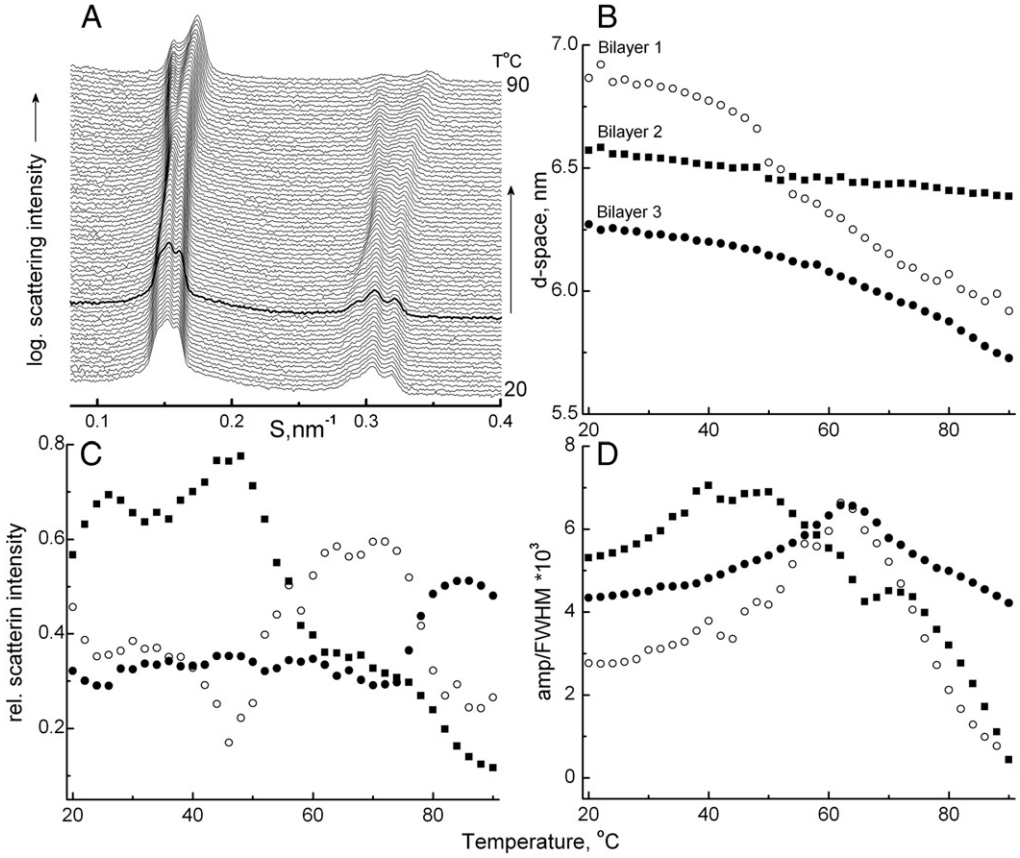

Fig. 1. Bilayer structures in ternary lipid dispersions depend on temperature. A. Overview of X-ray scattering intensity profiles in the region of the first two orders of lamellar repeats recorded from an aqueous dispersion of egg-SM:cholesterol:GlcCer in molar proportions 40:40:20 during a heating scan at 2°/min from 20 to 90 °C plotted on a logarithmic scale. The scattering intensity profile at 37 °C is highlighted. B. Three bilayer structures designated as Bilayer 1 (○), Bilayer 2 (■) and Bilayer 3 (●) indexed by 4-orders of reflection can be deconvolved from the Bragg peaks throughout the heating scan. C. Relative scattering intensities and D. Peak shape parameters (amplitude/full width at half maximum amplitude) of the deconvolved peaks from the first-order lamellar repeats are plotted as a function of temperature.

needle, sealed under argon, and annealed by 50 thermal cycles between −20 and 95 °C ensuring a complete mixing of lipids. The samples were stored under argon at a temperature not below 4 °C for at least 1 week before examination. X-ray diffraction examination was performed on samples equilibrated at 20 °C for 5 h before transfer into the measurement cell. In order to check for possible dehydration or demixing of the components various control measurements were undertaken such as checking for reversibility of phase behaviour during subsequent heating and cooling cycles. The samples were also checked for the absence of small- and wide-angle X-ray scattering regions for diffraction peaks from subgel or crystal phases of cholesterol and GluCer.

2.3. Synchrotron X-ray diffraction methods

X-ray diffraction measurements were performed at Station 2.1 of the Daresbury Synchrotron Radiation Source (Cheshire, UK). The X-ray wavelength was 0.154 nm with a beam geometry of ~1 × 2.5 mm. Simultaneous small-angle (SAXS) and wide-angle X-ray scattering (WAXS) intensities were recorded so that a correlation could be established between the mesophase repeat spacings and the packing arrangement of acyl chains. The SAXS intensity was recorded on a RAPID-2 detector [23] and 1-D scattering intensities were obtained by integration of a segment of the powder pattern. The Bragg spacings were calibrated using wet rat-tail collagen (67 nm [24]). The sample to detector distance was 1.5 m. The wide-angle scattering intensity was recorded with a HOTWAXS detector calibrated using the diffraction peaks from high-density polyethylene [25]. Lipid dispersions (20 μl) were sandwiched between two thin mica windows 0.5 mm apart and the measurement cell was mounted on a programmable temperature stage (Linkam, Surrey, UK). The temperature was monitored by a thermocouple inserted directly into the lipid dispersion (Quad Service, Poissy, France). The setup, calibration, and facilities available on Station 2.1 are described elsewhere [26]. Data reduction and analysis were performed using OriginPro8 software (OriginLab Corp.).

2.4. Analysis of X-ray diffraction data

The small angle X-ray scattering intensity profiles were analyzed using standard procedures [27]. Polarization and geometric corrections for line-width smearing were assessed by checking the symmetry of diffraction peaks in the present camera configuration using a sample of silver behenate (d = 5.838 nm). The orders of reflection could all be fitted by Voigt functions with fitting coefficients greater than $R^2 = 0.99$. Deconvolution is consistent with the sample to detector distance used [28]. Deconvolution of the SAXS and WAXS intensity peaks was undertaken using PeakFit (v4.12; Systat Software Inc.) software. Background subtraction was performed on each diffraction band but no corrections for polarization or geometric factors were necessary with the camera configuration employed.

3. Results

3.1. Bilayer structures in ternary lipid mixtures are temperature-dependent

The structure and distribution of lipids in bilayers observed in aqueous dispersions of ternary mixtures of egg-sphingomyelin (egg-SM), glucosylceramide (GlcCer) and cholesterol are temperature dependent. Fig. 1 shows an analysis of X-ray scattering intensities in the small-angle region (1.6–2.5°) of an equimolar mixture of egg-SM and cholesterol containing 20 mol% GlcCer during a heating scan from 20 to 90 °C at $2°\cdot min^{-1}$. Two sets of Bragg reflections representing the first and second orders of three coexisting bilayer structures are seen throughout the scan (Fig. 1A). The lamellar d-spacings of bilayers designated as bilayers 1 and 3 decrease during the scan while that of bilayer 2 is temperature independent (Fig. 1B).

A redistribution of lipid, judged by changes in relative scattering intensities of the bilayers (Fig. 1C), takes place between bilayers 1 and 2 in the temperature range 40–45 °C and in bilayer 3 at 73 °C coincident with the gel to fluid transition of egg-SM and GlcCer,

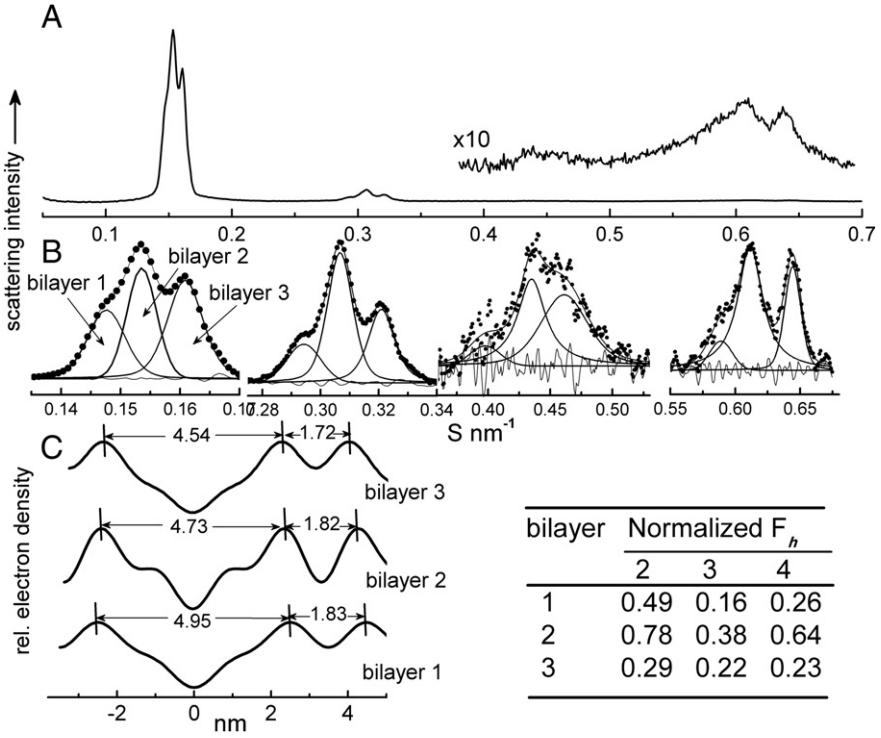

bilayer	Normalized F_h		
	2	3	4
1	0.49	0.16	0.26
2	0.78	0.38	0.64
3	0.29	0.22	0.23

Fig. 2. Structural determination of coexisting bilayers. Structure of coexisting bilayers in a ternary lipid mixture of egg-SM–cholesterol–GlcCer in molar proportions 40:40:20 at 37 °C. A. Scattering intensity profile showing four-orders of a lamellar structure with the third and fourth orders scaled by a factor of 10. B. Deconvolution of three bilayer structures by fits of Voigt-area functions to the first four orders of Bragg reflections. Residual errors are also shown by the light lines on each of the fitted curves. C. Relative electron density profiles of each bilayer structure calculated from the first four orders of lamellar reflection. The table shows form factors for orders $h = 2$, 3 & 4 normalized to F1 for each of the three bilayer structures.

respectively. This is associated with an increase in order within the respective unit cells seen in the changes of peak shape parameter, amplitude/full width at half maximum intensity (Fig. 1D), during heating to about 60 °C above which the unit cells become more disordered. Because each unique bilayer is characterized by a single set of Bragg reflections all three bilayers are coupled and in register across the bilayer.

3.2. The structure of coexisting bilayers

The structure of coexisting bilayers was assessed at 37 °C to model the physiological conditions under which these lipids are assembled into rafts. Structural parameters of the coexisting bilayers in the mixture shown in Fig. 1 were determined by calculation of relative electron density profiles through the bilayer repeats. Fig. 2A shows the scattering intensity profiles of the first four orders of lamellar repeat structures. Peak fitting methods were applied to lamellar Bragg reflections as illustrated for each of the reflections in Fig. 2B. There is a satisfactory fit of three Voigt-area functions to each Bragg peak as judged by the residual errors. Relative electron density profiles were calculated from the first four orders of reflection and the results are summarised in Fig. 2C. It can be seen that each bilayer has a unique structure as indicated by the differences in the structural parameters and normalized form factors and hence must be comprised of different lipid compositions.

3.3. The lipid composition of coexisting bilayers

The initial assignment of lipid composition of coexisting bilayers was made from X-ray scattering intensities recorded at small angles. Plots of the first-order scattering intensities recorded from equimolar mixtures of egg-SM and cholesterol containing different mol% GlcCer are shown in Fig. 3A. Coexisting bilayer structures are also observed in the absence of GlcCer indicating inhomogeneity in the distribution of sphingomyelin and cholesterol which is dependent on temperature [29] (Supplementary Fig. S1). The presence of only 2 mol% GlcCer results in a marked change in the bilayer structures such that two additional bilayers, designated as bilayer 1 and bilayer 3, are created in mixtures containing up to 20 mol% GlcCer. A collation of relative electron density calculations for all coexisting bilayers observed in mixtures containing 2 to 20 mol% GlcCer is presented in Table 1. In mixtures containing more than 20 mol% GlcCer only two coexisting bilayers are seen in the temperature range 20–73 °C which have different structural and thermotropic properties (Supplementary Fig. S2). The normalized deconvolved scattering intensities from the lamellar reflections are plotted as a function of the mass fraction of GlcCer in the mixtures in Fig. 3B. The values have been corrected for the angular-dependence of scattering intensity (Supplementary Fig. S3) and represent the relative mass of lipid in each of the bilayers. The method of correction was validated by the close correlation between relative scattering intensities of the first and second-order reflections (Supplementary Fig. S4). The amount of lipid in bilayer 1 increases with increasing proportion of GlcCer in the mixture and the

Table 1
Structural parameters of coexisting bilayers in aqueous dispersions of equimolar mixtures of egg-SM and cholesterol containing 2, 5, 10 and 20 mol% GlcCer at 37 °C.

	d-Space	d_{pp}	d_w
Bilayer 1	6.79 ± .01	4.95 ± .04	1.83 ± .05
Bilayer 2	6.55 ± .02	4.73 ± .04	1.82 ± .02
Bilayer 3	6.26 ± .03	4.54 ± .03	1.72 ± .04
SM:GlcCer 1:1	6.74 ± .07	4.86 ± .05	1.89 ± .02

Mean values ± SEM of bilayers deconvolved from all four ternary lipid mixtures and calculated from the first four orders of reflection of each bilayer. ANOVAR showed differences between the d-space and thickness for the three bilayers ($P < 0.001$) but no significant differences in d_w. Structural parameters of the SM–GlcCer complex were calculated from deconvolution of bilayers from three independent scattering intensity profiles from each of binary mixtures of egg-SM containing 5, 10 and 20 mol% GlcCer at 37 °C (Fig. S5). d-Space; lamellar repeat; d_{pp}; bilayer thickness: d_w; water layer thickness. t-Test comparisons showed no significant differences for any structural parameters between bilayer 1 and the complex of egg-SM and GlcCer.

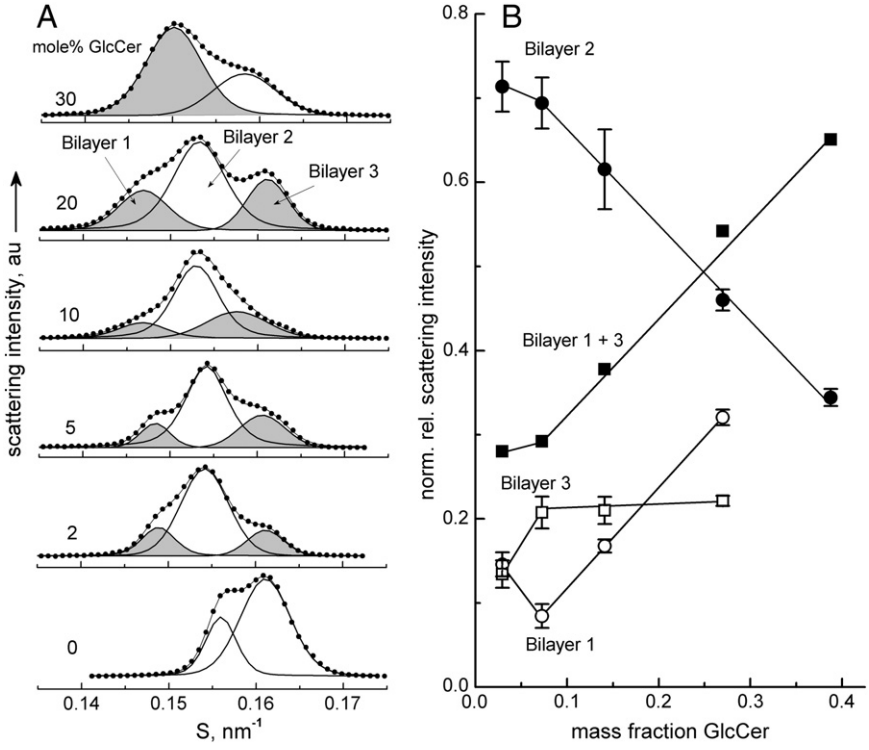

Fig. 3. Assignment of bilayer composition in ternary lipid mixtures from small-angle scattering. A. X-ray scattering intensity profiles in the region of the first-order lamellar Bragg reflections recorded from aqueous dispersions of ternary lipid mixtures comprised of equimolar mixtures of egg-SM and cholesterol containing indicated mol% GlcCer at 37 °C. B. Normalized relative scattering intensities of the first and second-order lamellar structures of bilayers identified in A, corrected for angular dependence of scattering intensity, plotted as a function of the mass fraction of GlcCer in the mixture. Values are means ± SEM of the first and second-order reflections of 6 independent diffraction patterns.

amount of lipid in bilayer 3 changes abruptly at 73 °C (Fig. 1C) indicating that these two bilayers contain GlcCer.

Egg-SM and GlcCer are known to form stoichiometric complexes of 1:1 at 30 °C and 2:1 at 50 °C [30]. At 37 °C the stoichiometry was found to be equimolar (Supplementary Fig. S5). A deconvolution of the first-order scattering intensity profile of a binary mixture of egg-SM and GlcCer in molar proportion 80:20 is shown in Fig. 4A and the calculated relative electron densities through the unit cells of the two structures are presented in Fig. 4B. The mean structural parameters obtained from the 1:1 stoichiometric complexes of binary mixtures that comprised of egg-SM containing 5, 10 and 20 mol% GlcCer are indistinguishable, within experimental error, from those of bilayer 1 (Table 1) and this defines the composition of bilayer 1. The amount of egg-SM and GlcCer in bilayer 1 can therefore be calculated from the relative scattering intensities in Fig. 3B (Supplementary Section 6). Bilayer 1 in ternary mixtures containing 5, 10 and 20 mol% GlcCer was found to contain 63.2 ± 0.5% of the total GlcCer present in each of these mixtures. An explanation for the distribution of GlcCer between bilayer 1 and the other bilayer structures resides in the spectrum of molecular species of glucocerebroside present in the extract (Supplementary Table S1). Cerebrosides with N-acyl chains longer than 20 carbons represent about two thirds of the molecular species of GlcCer with the remainder having chains more or less symmetric with the sphingosine moiety. This assignment is consistent with the difference in bilayer thickness between bilayers 1 and 3 and the volume of hydrocarbon forming complexes with symmetric and asymmetric molecular species of GlcCer (Supplementary Section 6).

The distribution of lipids between bilayers 2 and 3 can be obtained from an analysis of the wide-angle (7.3–11.1°) scattering profiles recorded from the ternary mixtures at 37 °C (Fig. 5A). An equimolar mixture of egg-SM and cholesterol produces a broad wide-angle reflection centred at a spacing of 0.495 ± 0.003 nm which has been shown by

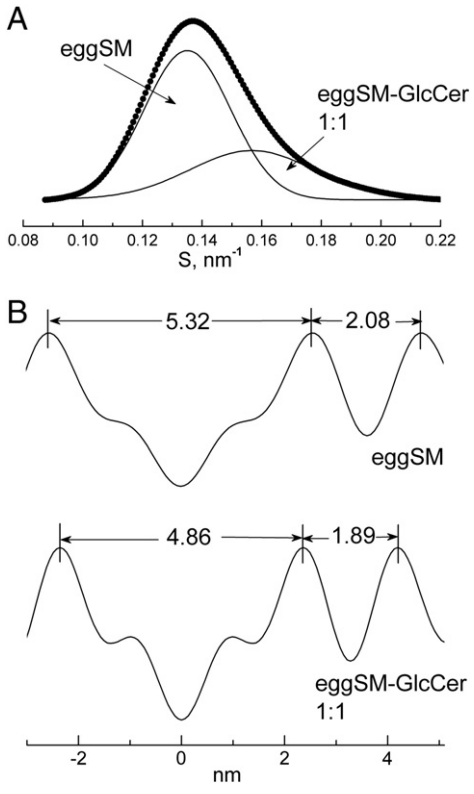

Fig. 4. Structure of egg-SM complex with GlcCer. A. Deconvolution of the scattering intensity profile of the first-order Bragg reflection of a binary mixture of egg-SM and GlcCer in molar proportion 80:20 at 37 °C. B. Relative electron densities calculated through the unit cells of coexisting bilayers in A.

electron spin resonance probe methods to be a liquid-ordered structure [31]. An additional reflection is observed in all ternary mixtures at a d-spacing of 0.447 ± 0.003 nm assigned as hydrocarbon chains packed in an hexagonal configuration with an interchain spacing of 0.52 nm, intermediate between gel (0.48 nm) and fluid (0.55 nm) structures. This structure in stoichiometric complexes of phospholipid and GlcCer has the properties of a liquid-ordered phase as judged by electron spin resonance probe measurements [32]. A plot of the relative scattering intensities of the peak at 0.447 nm as a function of the mass fraction of GlcCer in the ternary lipid mixtures is shown in Fig. 5B. Since the mass of asymmetric GlcCer and egg-SM in bilayer 1 can be determined for each of the ternary mixtures (Supplementary Section 6) the contribution to the relative scattering intensity of the WAXS peak centred at a d-spacing of 0.447 nm from bilayer 1 can be calculated. It can be seen that the intensity of the scattering from the peak at 0.447 nm is greater than can be accounted for by bilayer 1. A plot of this additional intensity against the mass fraction of GlcCer (Fig. 5C) coincides with the corresponding relative intensities of bilayer 3 observed in mixtures containing 2–20 mol% GlcCer indicating that bilayer 3 is comprised only of symmetric molecular species of GlcCer and egg-SM. Accordingly, bilayer 2 must contain only egg-SM and cholesterol. This is consistent with the close relationship between the relative scattering intensities of the wide-angle scattering peak at 0.495 nm and the relative scattering intensity bilayer 2 in Fig. 3B assigned as a liquid-ordered structure of egg-SM and cholesterol (Fig. 5C).

The relative scattering intensity of bilayer 3 remains fairly constant in ternary mixtures containing up to 20 mol% GlcCer. Since the amount of symmetric GlcCer increases proportionately to the total mass of GlcCer in the mixture there must be a corresponding decrease in the amount of egg-SM in bilayer 3. Knowing the amount of symmetric GlcCer in the ternary lipid mixtures and the total mass of lipid in bilayer 3 the amount of egg-SM in each of the ternary mixtures can be calculated. An exponential relationship is found between the ratio of egg-SM: GlcCer in bilayer 3 and the mass fraction of GlcCer in the mixtures (Fig. 6). This shows that when the proportion of GlcCer in the ternary mixture exceeds about 28 mol% the stoichiometry of egg-SM:GlcCer is less than 1:1. Under these conditions cholesterol mixes with bilayers containing GlcCer.

3.4. Distribution of lipids in mixtures with proportions of GlcCer greater than 20 mol%

The difference between the total amount of egg-SM in the ternary mixtures and the amounts of egg-SM in bilayers 1 and 3 is the amount of egg-SM in bilayer 2. Bilayers 1 and 3 are devoid of cholesterol hence bilayer 2 is found to be comprised of egg-SM containing 66 mol% cholesterol which is known to be a saturating amount in liquid-ordered bilayers of egg-SM [33]. The formation of two bilayer structures in ternary lipid mixtures containing 30 mol% GlcCer occurs when an equimolar stoichiometry of egg-SM and GlcCer cannot be maintained without removal of additional egg-SM from bilayer 2. An analysis of the structure and composition of the two bilayers is presented in Fig. 7. The scattering intensity profile of the first-order Bragg reflection of a ternary lipid mixture containing 30 mol% GlcCer at 37 °C can be deconvolved into two coexisting bilayer structures (Fig. 7A). Peak 2 is designated as bilayers of egg-SM containing 66 mol% cholesterol. Relative electron density profiles calculated from the first four orders of reflection of the bilayer repeats (Fig. 7B) indicate that the structure of the bilayers is different from that of the bilayers observed in the mixtures containing 2–20 mol% GlcCer presumably because the redistribution of the three lipids is different. A tentative composition of the two bilayers based on the scattering data in Fig. 3B is shown in Fig. 7C. According to this analysis the lamellar structure designated as peak 2 is comprised largely of egg-SM and cholesterol while some cholesterol and egg-SM have redistributed to form peak 1 which contains the GlcCer (Fig. 7C).

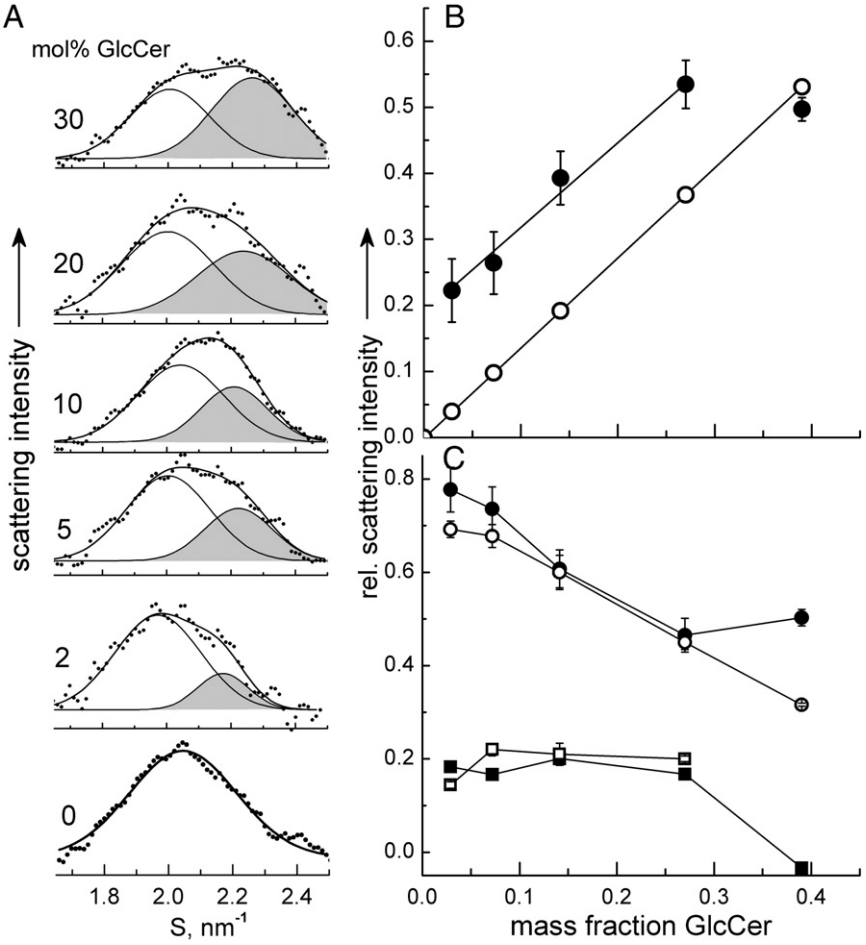

Fig. 5. Assignment of bilayer composition in ternary lipid mixtures from wide-angle scattering. A. X-ray scattering intensity profiles recorded in the wide-angle region from aqueous dispersions of ternary lipid mixtures comprised of equimolar mixtures of egg-SM and cholesterol containing the indicated mol% GlcCer at 37 °C. The intensity profiles from 4 independent recordings were deconvolved by fits of two Voigt-area functions giving d-spacings of 0.495 ± 0.003 and 0.447 ± 0.003 nm, respectively. B. Relative scattering intensity of the shaded peak in A plotted as a function of the mass fraction of GlcCer in the mixture (●). Calculated relative scattering intensities from equimolar complexes of egg-SM and asymmetric GlcCer comprising bilayer 1 are also shown (○). C. Plot of relative scattering intensities of bilayer 2 in Fig. 2B (○) and the peak of d-spacing 0.495 nm in A (●). Values are mean ± SEM of 4 measurements. Plot of the difference in scattering intensities shown in B (■). Relative scattering intensities of bilayer 3 in Fig. 2B (□).

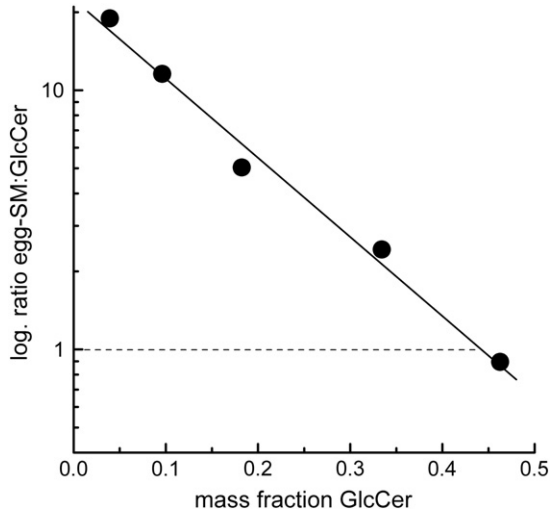

Fig. 6. Composition of bilayer 3. Plot of the ratio egg-SM:GlcCer in bilayer 3 as a function of mass fraction of GlcCer in the ternary lipid mixtures.

4. Discussion

The model studies reported here are not in agreement with current theories of lipid domain formation in membranes. The distribution of lipids in what are often referred to as canonical raft mixtures are seen to be dominated by the glycosphingolipids and in particular the molecular species of glycosphingolipid determined by the length of the N-acyl fatty acid of the ceramide. The effect of cholesterol in the mixtures examined acts simply to limit the amount of phospholipid able to interact with the glycosphingolipid to that in excess of the amount required to prevent an energetically unfavourable crystallization of cholesterol. It is also evident that in proportions of glycosphingolipids found in biological membranes gel phase separation is avoided by formation of complexes with membrane phospholipids despite having phase transition temperatures well above the physiological range.

A collation of available data on the lipid composition of rafts isolated from biological membranes shows that the proportion of glycerophospholipids is at least twice that of sphingomyelin [34]. This raises the question of how glycerophosphatidylcholine might compete with sphingomyelin for interaction with cholesterol and glycosphingolipids in membranes. The present results can provide a guide to the interpretation of data using conventional X-ray diffraction methods reported previously for similar ternary mixtures in which dipalmitoylphosphatidylcholine replaced egg-SM [16]. At temperatures less that 50 °C a proportion of 22 mol% glycosphingolipid was

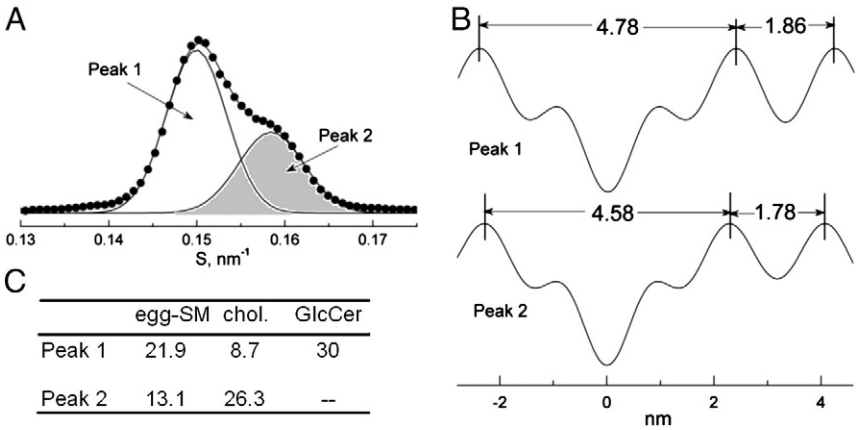

C

	egg-SM	chol.	GlcCer
Peak 1	21.9	8.7	30
Peak 2	13.1	26.3	--

Fig. 7. Structure and tentative composition of coexisting bilayers in ternary lipid mixture containing 30 mol% GlcCer at 37 °C. A. Deconvolution of two bilayer structures from the first-order Bragg reflection. B. Relative electron density profiles through the bilayer repeat structure calculated from the first four orders of reflection for peaks designated as 1 & 2. C. Tentative lipid composition of peaks 1 & 2.

incorporated into an equimolar phospholipid–cholesterol mixture. It is known that dipalmitoylphosphatidylcholine forms a 1:1 complex with GlcCer [35] and formation of bilayers of this complex would produce another bilayer of phospholipid containing 65 mol% cholesterol. The difference between ternary mixtures containing egg-SM and dipalmitoylphosphatidylcholine is seen when the proportion of glycosphingolipid is present in excess of 20 mol%. Thus cholesterol and egg-SM are incorporated into GlcCer-rich bilayers (Fig. 7) but excess glycosphingolipid forms bilayers of pure lipid in gel phase in mixtures with glycerophospholipid. This indicates that glycosphingolipid can accommodate some cholesterol only if accompanied by sphingomyelin but not by phosphatidylcholine suggesting that glycosphingolipid forms tighter complexes with sphingomyelin than with saturated glycerophospholipid.

The results reported here provide a rational basis for understanding the specificity associated with different membrane raft functions. It is clear that the involvement of glycosphingolipids in signalling processes involves not only the class of sphingolipid defined by the type of sugar residue and the molecular species defined by the length and type of N-acyl fatty acid residue of the ceramide but also their lateral arrangement and coupling with appropriate domains on the opposing bilayer leaflet. While there is evidence favouring lateral segregation of glycosphingolipids like GM1 in the conduct of their signalling function [36] there are differences of opinion about how this may be achieved. One model envisages that complex glycosphingolipids are phase separated into gel phase domains driven by their relatively high order-disorder phase transition temperature while simple glycosphingolipids such as galactosy- and glucosylceramides form liquid-ordered phases with cholesterol [18]. Another model describes a phase separation of complex glycosphingolipids based on steric hindrance of bulky sugar groups segregating them into regions of high membrane curvature [37]. Both models appear implausible on the basis of the present results. Cholesterol does not interact with either symmetric or asymmetric glycosphingolipid and there is no evidence in the wide-angle scattering region of gel phases at any temperature down to 20 °C in the mixtures examined. Recent studies using secondary ion mass spectrometry have, however, reported evidence that cholesterol induces a phase separation of ganglioside GM1 into nanoscale assemblies rich in sphingomyelin [38]. The present results show that cholesterol increases order within the unit cells of eggSM:GlcCer complexes (Supplementary Fig. S5) suggesting that cholesterol, while clearly not a component of the complex, is closely associated with them and may represent one of the roles of cholesterol in membrane lipid raft assembly. With regard to phase separation models reliant on the steric hindrance between bulky polar groups it is unlikely that this will be a factor when the glycosphingolipid is complexed with phospholipid. Furthermore, all mixtures examined in this study form smectic mesophases with no evidence of diffuse scattering from bilayers with low radii of curvature. The creation of glycosphingolipid–phospholipid liquid-ordered complexes will result in display of sugar residues on the membrane surface in a hexagonal array in the case of asymmetric molecular species and in less regular, quasi-crystalline configurations with symmetric molecular species which would depend on the precise proportions of the two lipids in the structure.

X-ray diffraction methods give no information on the lateral dimensions of membrane domains, however, to act in dynamic processes they are likely to be relatively small and consist of assemblies of at most tens of molecules rather than extensive static phases. By contrast, the method provides conclusive evidence that the domains are strongly coupled and in register across the bilayers in these model membrane systems. The lipids and proteins of biological membranes, however, are asymmetrically arranged and this asymmetry appears to be exploited in the execution of transient functions including those of raft-associated signalling processes. Defining the interplay of forces required to couple domains on either side of cell membranes remains a considerable challenge but molecular species asymmetry could contribute to these forces. The interdigitation or residence of the terminal ends of the long N-acyl chains comprising asymmetric ceramides in the central plane of lipid bilayers has long been mooted as a coupling mechanism [39]. More recently, neutron scattering studies of GM1-containing asymmetric bilayers indicate that coupling to cholesterol in the opposing leaflet takes place [40] and providing further confirmation that cholesterol does not mix with glycosphingolipids in these model systems. The situation in biological membranes is obviously more complicated because there is evidence that asymmetric glucosylceramide is located on the cytoplasmic side of the plasma membrane where it is likely to form stoichiometric complexes with phosphatidylethanolamines capable of registering with asymmetric glycosphingolipid domains on the cell surface [34] but in any event cholesterol is excluded from these complexes.

A number of conclusions can be drawn from the present results that are pertinent to the role of lipids in the formation of membrane rafts. The stoichiometry of sphingomyelin and cholesterol in rafts present in cell membranes will depend critically on the amount of symmetric molecular species of sphingomyelin that is not sequestered into complexes with glycosphingolipids. Clearly cholesterol is not the primary driving force for the creation of lipid domains into which raft-associated proteins are incorporated. An alternative mode of assembly of functional cholesterol-containing rafts may be accomplished by coalescence of raft proteins which interact with raft lipids at specific sites on their transmembrane segments. Many raft-associated proteins possess cholesterol recognition/interaction amino acid consensus (CRAC; CARC)

motifs [41,42] while a motif for specific binding of symmetric sphingomyelin (C-18:0) to coat-protein complex I (COPI) has been described [43]. Covalent binding of cholesterol anchors is known to be a feature of hedgehog signalling [44].

Another inference that can be made concerns the binding of pentavalent toxins such as cholera and *Shigella* toxins and polyomaviruses to their particular glycosphingolipid receptors. Binding to symmetric rather than asymmetric molecular species is likely to be favoured although less infective variants that bind to asymmetric glycosphingolipids have been reported [45]. This is because asymmetric ceramide lipids form strictly 1:1 stoichiometric complexes with choline phospholipids and pack laterally in the bilayer in hexagonal array whereas symmetric glycosphingolipids can assemble in quasi-crystalline configurations of 1:1.6 stoichiometry with phospholipid to form an array with 5-fold symmetry exemplified by Penrose tiles. This is an important consideration as retrograde transport of the toxin–receptor complex is achieved only on binding to symmetric molecular species of glycosphingolipid. In the case of cholera toxin binding to GM1 the N-acyl chain must be mono-unsaturated or relatively short to enter retrograde [46,47] or transcytotic [48] pathways. Likewise, entry of SV40 virions into host cells requires binding to symmetric molecular species of GM1 [49].

The function of asymmetric glycosphingolipids appears to be largely concerned with cell signalling and development [18]. They are also known to be key players in a variety of disease states including glycolipid lysosomal storage, infectious and neurodegenerative diseases, cancer and diabetes [50,51]. Biosynthesis of asymmetric GlcCer is geared to that of GPI anchors [52] suggesting that functional interactions take place in membrane rafts. Their role in transmembrane signalling processes has been clearly demonstrated in experiments where the consequences of varying the length of the N-acyl chain of glycosphingolipids have been examined [17,53–55]. The complexity of known molecular species of asymmetric glycosphingolipids, which vary both in the ceramide and sugar constituents, is in keeping with the multitude of tasks with which they have been associated. With the application of increasingly sophisticated methods of analysis exploiting both physical and biochemical properties of the lipids [56] a clearer picture of their particular role in cell signalling is emerging.

Acknowledgements

I thank G. Grossman for the assistance in setting up the SRS station, C. Wolf and G. Staneva for the help with data collection and H. Takahashi for the comments on the manuscript.

Appendix A. Supplementary data

Supplementary data to this article can be found online at http://dx.doi.org/10.1016/j.bbamem.2014.02.021.

References

[1] T.T. Sebastian, R.D. Baldridge, P. Xu, T.R. Graham, Phospholipid flippases: building asymmetric membranes and transport vesicles, Biochim. Biophys. Acta 1821 (2012) 1068–1077.
[2] V. Mueller, A. Honigmann, C. Ringemann, R. Medda, G. Schwarzmann, C. Eggeling, FCS in STED microscopy: studying the nanoscale of lipid membrane dynamics, Methods Enzymol. 519 (2013) 1–38.
[3] J.M. Kwiatek, D.M. Owen, A. Abu-Siniyeh, P. Yan, L.M. Loew, K. Gaus, Characterization of a new series of fluorescent probes for imaging membrane order, PLoS One 8 (2013) 7.
[4] J. Fantini, F.J. Barrantes, How cholesterol interacts with membrane proteins: an exploration of cholesterol-binding sites including CRAC, CARC and tilted domains, Front. Physiol. 4 (2013) 1–9.
[5] H. Keller, H.-G. Kraeusslich, P. Schwille, Multimerizable HIV Gag derivative binds to the liquid-disordered phase in model membranes, Cell. Microbiol. 15 (2013) 237–247.
[6] K. Simons, E. Ikonen, Functional rafts in cell membranes, Nature 387 (1997) 569–572.
[7] D. Lingwood, K. Simons, Lipid rafts as a membrane-organizing principle, Science 327 (2010) 46–50.
[8] J.F. Hancock, Lipid rafts: contentious only from simplistic standpoints, Nat. Rev. Mol. Cell Biol. 7 (2006) 456–462.
[9] J. Malinsky, M. Opekarova, G. Grossmann, W. Tanner, Membrane microdomains, rafts, and detergent-resistant membranes in plants and fungi, Annu. Rev. Plant Biol. 64 (2013) 501–529.
[10] S. Jaikishan, J.P. Slotte, Effect of hydrophobic mismatch and interdigitation on sterol/sphingomyelin interaction in ternary bilayer membranes, Biochim. Biophys. Acta 1808 (2011) 1940–1945.
[11] T.N. Estep, D.B. Mountcastle, Y. Barenholz, R.L. Biltonen, T.E. Thompson, Thermal behaviour of synthetic sphingomyelin–cholesterol dispersions, Biochemistry 18 (1979) 2112–2117.
[12] P.J. Quinn, Lipid–lipid interactions in bilayer membranes: married couples and casual liaisons, Prog. Lipid Res. 51 (2012) 179–198.
[13] A.M. Ernst, F.-X. Contreras, C. Thiele, F. Wieland, B. Bruegger, Mutual recognition of sphingolipid molecular species in membranes, Biochim. Biophys. Acta 1818 (2012) 2616–2622.
[14] P.J. Quinn, C. Wolf, Egg-sphingomyelin and cholesterol form a stoichiometric molecular complex in bilayers of egg-phosphatidylcholine, J. Phys. Chem. B 114 (2010) 15536–15545.
[15] P.J. Quinn, Structure of sphingomyelin bilayers and complexes with cholesterol forming membrane rafts, Langmuir 29 (2013) 9447–9456.
[16] M.J. Ruocco, G.G. Shipley, Interaction of cholesterol with galactocerebroside and galactocerebroside-phosphatidylcholine bilayer membranes, Biophys. J. 46 (1984) 695–707.
[17] K. Iwabuchi, H. Nakayama, C. Iwahara, K. Takamori, Significance of glycosphingolipid fatty acid chain length on membrane microdomain-mediated signal transduction, FEBS Lett. 584 (2010) 1642–1652.
[18] S.M. Pontier, F. Schweisguth, Glycosphingolipids in signaling and development: from liposomes to model organisms, Dev. Dyn. 241 (2012) 92–106.
[19] J.F. Frisz, H.A. Klitzing, K. Lou, I.D. Hutcheon, P.K. Weber, J. Zimmerberg, M.L. Kraft, Sphingolipid domains in the plasma membranes of fibroblasts are not enriched with cholesterol, J. Biol. Chem. 288 (2013) 16855–16861.
[20] X. Chen, M.J. Lawrence, D.J. Barlow, R.J. Morris, R.K. Heenan, P.J. Quinn, The structure of detergent-resistant membrane vesicles from rat brain cells, Biochim. Biophys. Acta 1788 (2009) 477–483.
[21] G.W. Feigenson, Phase boundaries and biological membranes, Annu. Rev. Biophys. Biomol. Struct. 36 (2007) 63–77.
[22] F.M. Goni, A. Alonso, L.A. Bagatolli, R.E. Brown, D. Marsh, M. Prieto, J.L. Thewalt, Phase diagrams of lipid mixtures relevant to the study of membrane rafts, Biochim. Biophys. Acta 1781 (2008) 665–684.
[23] R. Lewis, I. Sumner, A. Berry, J. Bordas, A. Gabriel, G. Mant, B. Parker, K. Roberts, J. Worgan, Multiwire X-ray detector systems at the Daresbury SRS, Nucl. Instrum. Methods Phys. Res. A 273 (1988) 773–777.
[24] A. Bigi, L. Dovigo, M.H.J. Koch, M. Morocutti, A. Ripamonti, N. Roveri, Collagen structural organisation in uncalcified and calcified human anterior longitudinal ligament, Connect. Tissue Res. 25 (1991) 171–179.
[25] E.J. Addink, J. Beintema, Polymorphism of crystalline polypropylene, Polymer 2 (1961) 185–193.
[26] E. Towns-Andrews, A. Berry, J. Bordas, G.R. Mant, P.K. Murray, K. Roberts, I. Sumner, J.S. Worgan, R. Lewis, A. Gabriel, Time-resolved X-ray diffraction station — X-ray optics, detectors and data acquisition, Rev. Sci. Instrum. 60 (1989) 2346–2349.
[27] R.T. Zhang, R.M. Suter, J.F. Nagle, Theory of the structure factor of lipid bilayers, Phys. Rev. E. 50 (1994) 5047–5060.
[28] T. Yao, H. Jinno, Polarization factor for the X-ray powder diffraction method with a single crystal monochromator, Acta Crystallogr. A 38 (1982) 287–288.
[29] P.J. Quinn, C. Wolf, Thermotropic and structural evaluation of the interaction of natural sphingomyelins with cholesterol, Biochim. Biophys. Acta 1788 (2009) 1877–1889.
[30] P.J. Quinn, A synchrotron X-ray diffraction characterization of the structure of complexes formed between sphingomyelin and cerebroside, FEBS J. 278 (2011) 3518–3527.
[31] G. Staneva, C. Chachaty, C. Wolf, P.J. Quinn, Comparison of the liquid-ordered bilayer phases containing cholesterol or 7-dehydrocholesterol in modeling Smith–Lemli–Opitz syndrome, J. Lipid Res. 51 (2010) 1810–1822.
[32] Y. Feng, D. Rainteau, C. Chachaty, Z.W. Yu, C. Wolf, P.J. Quinn, Characterization of a quasicrystal line phase in codispersions of phosphatidylethanolamine and glucocerebroside, Biophys. J. 86 (2004) 2208–2217.
[33] L. Mainali, M. Raguz, W.K. Subczynski, Phases and domains in sphingomyelin–cholesterol membranes: structure and properties using EPR spin-labeling methods, Eur. Biophys. J. Biophys. Lett. 41 (2012) 147–159.
[34] P.J. Quinn, A lipid matrix model of membrane raft structure, Prog. Lipid Res. 49 (2010) 390–406.
[35] P.J. Quinn, Long N-acyl fatty acids on sphingolipids are responsible for miscibility with phospholipids to form liquid-ordered phase, Biochim. Biophys. Acta 1788 (2009) 2267–2276.
[36] R. Jennemann, H.-J. Groene, Cell-specific in vivo functions of glycosphingolipids: lessons from genetic deletions of enzymes involved in glycosphingolipid synthesis, Prog. Lipid Res. 52 (2013) 231–248.
[37] S. Sonnino, A. Prinetti, Lipids and membrane lateral organization, Front. Physiol. 1 (2010) 153.
[38] M.M. Lozano, Z. Liu, E. Sunnick, A. Janshoff, K. Kumar, S.G. Boxer, Colocalization of the ganglioside G(M1) and cholesterol detected by secondary ion mass spectrometry, J. Am. Chem. Soc. 135 (2013) 5620–5630.
[39] D.A. Pantano, P.B. Moore, M.L. Klein, D.E. Discher, Raft registration across bilayers in a molecularly detailed model, Soft Matter 7 (2011) 8182–8191.

[40] V. Rondelli, G. Fragneto, S. Motta, E. Del Favero, P. Brocca, S. Sonnino, L. Cantu, Ganglioside GM1 forces the redistribution of cholesterol in a biomimetic membrane, Biochim. Biophys. Acta 1818 (2012) 2860–2867.
[41] C. Schroeder, Cholesterol-binding viral proteins in virus entry and morphogenesis, Subcell. Biochem. 51 (2010) 77–108.
[42] M. Jafurulla, A. Chattopadhyay, Membrane lipids in the function of serotonin and adrenergic receptors, Curr. Med. Chem. 20 (2013) 47–55.
[43] F.X. Contreras, A.M. Ernst, P. Haberkant, P. Bjorkholm, E. Lindahl, B. Gonen, C. Tischer, A. Elofsson, G. von Heijne, C. Thiele, R. Pepperkok, F. Wieland, B. Brugger, Molecular recognition of a single sphingolipid species by a protein's transmembrane domain, Nature 481 (2012) 525–529.
[44] A.C. Gradilla, I. Guerrero, Hedgehog on the move: a precise spatial control of Hedgehog dispersion shapes the gradient, Curr. Opin. Genet. Dev. 23 (2013) 363–373.
[45] C.S. Berenson, H.F. Nawar, R.L. Kruzel, L.M. Mandell, T.D. Connell, Ganglioside-binding specificities of *E. coli* enterotoxin LT-IIc: importance of long-chain fatty acyl ceramide, Glycobiology 23 (2013) 23–31.
[46] D.J.F. Chinnapen, W.-T. Hsieh, Y.M. te Welscher, D.E. Saslowsky, L. Kaoutzani, E. Brandsma, L. D'Auria, H. Park, J.S. Wagner, K.R. Drake, M. Kang, T. Benjamin, M.D. Ullman, C.E. Costello, A.K. Kenworthy, T. Baumgart, R.H. Massol, W.I. Lencer, Lipid sorting by ceramide structure from plasma membrane to ER for the cholera toxin receptor ganglioside GM1, Dev. Cell 23 (2012) 573–586.
[47] H. Raa, S. Grimmer, D. Schwudke, J. Bergan, S. Walchli, T. Skotland, A. Shevchenko, K. Sandvig, Glycosphingolipid requirements for endosome-to-Golgi transport of Shiga toxin, Traffic 10 (2009) 868–882.
[48] D.E. Saslowsky, Y.M. te Welscher, D.J.-F. Chinnapen, J.S. Wagner, J. Wan, E. Kern, W.I. Lencer, GM1-mediated transcytosis of cholera toxin bypasses the retrograde pathway and depends on the structure of the ceramide domain, J. Biol. Chem. 288 (2013) 25804–25809.
[49] H. Ewers, W. Roemer, A.E. Smith, K. Bacia, S. Dmitrieff, W. Chai, R. Mancini, J. Kartenbeck, V. Chambon, L. Berland, A. Oppenheim, G. Schwarzmann, T. Feizi, P. Schwille, P. Sens, A. Helenius, L. Johannes, GM1 structure determines SV40-induced membrane invagination and infection, Nat. Cell Biol. 12 (2010) 11–18.
[50] A.H. Merrill Jr., Sphingolipid and glycosphingolipid metabolic pathways in the era of sphingolipidomics, Chem. Rev. 111 (2011) 6387–6422.
[51] Y.-H. Xu, S. Barnes, Y. Sun, G.A. Grabowski, Multi-system disorders of glycosphingolipid and ganglioside metabolism, J. Lipid Res. 51 (2010) 1643–1675.
[52] U. Loizides-Mangold, F.P.A. David, V.J. Nesatyy, T. Kinoshita, H. Riezman, Glycosylphosphatidylinositol anchors regulate glycosphingolipid levels, J. Lipid Res. 53 (2012) 1522–1534.
[53] D. Lingwood, B. Binnington, T. Rog, I. Vattulainen, M. Grzybek, U. Coskun, C.A. Lingwood, K. Simons, Cholesterol modulates glycolipid conformation and receptor activity, Nat. Chem. Biol. 7 (2011) 260–262.
[54] K. Iwabuchi, H. Nakayama, H. Masuda, K. Kina, H. Ogawa, K. Takamori, Membrane microdomains in immunity: glycosphingolipid-enriched domain-mediated innate immune responses, Biofactors 38 (2012) 275–283.
[55] J.W. Park, W.J. Park, Y. Kuperman, S. Boura-Halfon, Y. Pewzner-Jung, A.H. Futerman, Ablation of Very Long Acyl Chain Sphingolipids Causes Hepatic Insulin Resistance in Mice Due to Altered Detergent-Resistant Membranes, Hepatology 57 (2013) 525–532.
[56] I. Meisen, M. Mormann, J. Muthing, Thin-layer chromatography, overlay technique and mass spectrometry: a versatile triad advancing glycosphingolipidomics, Biochim. Biophys. Acta 1811 (2011) 875–896.